

# NMR Study of the Water Dynamics in Aqueous Colloidal Magnetic Fluids at Different pH's and Grains Concentrations

C. E. González,<sup>†</sup> D. J. Pusiol,<sup>‡</sup> A. M. Figueiredo Neto,<sup>\*,‡</sup> M. Ramia,<sup>†</sup> A. Bourdon,<sup>§</sup> and A. Bee<sup>||</sup>

Facultad de Matemática, Astronomía y Física, Universidad Nacional de Córdoba,  
Ciudad Universitaria 5000 Córdoba, Argentina, Instituto de Física, Universidade de São Paulo,  
caixa postal 66318, 05315-970 São Paulo, Brasil, LMDH Milieux Désordonnés et Hétérogènes,  
UMR 7603 du CNRS, Université Pierre et Marie Curie, case 86, 4 Place Jussieu,  
75252 Paris Cedex 05 France, and LI2C Colloides Inorganiques, UMR 7612 du CNRS,  
Université Pierre et Marie Curie, case 63, 4 Place Jussieu, 75252 Paris Cedex 05, France

Received: May 13, 2002; In Final Form: October 8, 2002

In a previous NMR study [González, C.E.; et al. *J. Chem. Phys.* **1998**, *109*, 4670] we observed that the <sup>1</sup>H and <sup>2</sup>H spectra of both surfacted and ionic ferrofluids are broad and asymmetric. In ionic ferrofluids, this effect could be due to (i) electric interactions between the electrically charged magnetic grains and the electric dipole moments of water molecules and/or (ii) the interaction between water molecules and the distribution of magnetic field gradients in the intergrain volume. In this work we study a series of ionic ferrofluids prepared at different magnetic grains concentrations and with different surface charge densities. Our experiments clearly show that the sign and the density of the electric charge of the magnetic grains have no influence on the NMR spectra. On the other hand, spectral widths increase with the magnetic grains concentration, all the samples being far from the motional narrowing regime.

## Introduction

Ferrofluids<sup>1</sup> are magnetic liquids in which magnetic iron oxide nanograins are dispersed in a liquid carrier. These complex fluids have interesting chemical and physical properties, yielding steadily growing applications.<sup>2</sup> Ferrofluids are classified in two groups, depending on the method used to avoid magnetic grain aggregation, namely ionic (IFF)<sup>3</sup> and surfacted (SFF)<sup>1</sup> ferrofluids. IFF<sup>3</sup> are made of charged magnetic grains dispersed in water in which electrostatic repulsion prevents macro-ions from aggregating. SFF are suspensions, in organic or inorganic solvents, of magnetic grains that are subjected to steric repulsion by means of a surfactant coating.

In a recent NMR study,<sup>4</sup> we compared the <sup>1</sup>H and <sup>2</sup>H spectra of the carrier water in both types of aqueous ferrofluids. They exhibit asymmetric line shapes similar to those given by a static distribution of magnetic dipoles placed in a disordered lattice, but the measured line width is 10 times smaller than that given by a completely static model. More precisely, these spectra are similar to those given by a model where water molecules are within the interstitial volume between magnetic grains, subjected to a magnetic field averaged on a sphere of about 20 Å in diameter. The volume of this sphere represents the region in which water molecules diffuse during each NMR measurement (about 50–500 μs).

In an effort to elucidate the origin of these widened spectra in IFF, we investigate if it is due to (i) the interaction of the water molecules with the local magnetic field gradient in the intergrains volume, as pointed out in ref 4, local magnetic field

gradients are of the order of  $2 \times 10^5 \text{ T m}^{-1}$  in the intergrain space or (ii) the restriction of the translational mobility of water molecules due to electrostatic interactions between charged grains and the (polar) water molecules.

To be able to choose between an electric origin and a magnetic one, we have taken profit of our ability of controlling some characteristics of the ionic magnetic colloidal suspension: grain size, pH (which controls the surface charge density), and grain concentration. In this paper we report an experimental study on <sup>1</sup>H NMR spectra in IFF and the time evolution of the Hahn echo amplitude at different pH values and different grain concentrations, whereas grain sizes are kept constant.

## Experimental Section

**A. Sample Preparation.** The magnetic liquids used here are ionic ferrofluids (IFF) made of magnetic nanograins of maghemite (γ-Fe<sub>2</sub>O<sub>3</sub>), dispersed in water. They are chemically synthesized according to a method described in ref 3. The mean crystalline diameter determined by X-ray diffraction is typically 8 nm. The stability of the ferrofluid is mainly ensured by electrostatic repulsion between charged grains. The pH value for the point of zero charge (PZC) is about 7.3 for maghemite grains. Near the PZC (5 < pH < 10) the surface charge density is low, electrostatic repulsion between grains is not strong enough, and ferrofluids flocculate. The pH domains for stability lie on both sides of the PZC vicinity, the surface charge being either positive (pH < PZC) or negative (pH > PZC).

*Different [Fe] at Constant pH Value.* Samples at different grain concentrations are prepared by dilution of ferrofluid in distillate water, whereas the pH value is kept constant by adding the appropriate volume of tetramethylammonium hydroxide (TMAOH). Two different pH values are chosen to study the influence of the sign of the surface charge: pH = 2.5, in this case grains bear positive charges with nitrate counterions (acid

<sup>†</sup> Universidad Nacional de Córdoba.

<sup>‡</sup> Universidade de São Paulo.

<sup>§</sup> LMDH Milieux Désordonnés et Hétérogènes, UMR 7603 du CNRS, Université Pierre et Marie Curie.

<sup>||</sup> LI2C Colloides Inorganiques, UMR 7612 du CNRS, Université Pierre et Marie Curie.

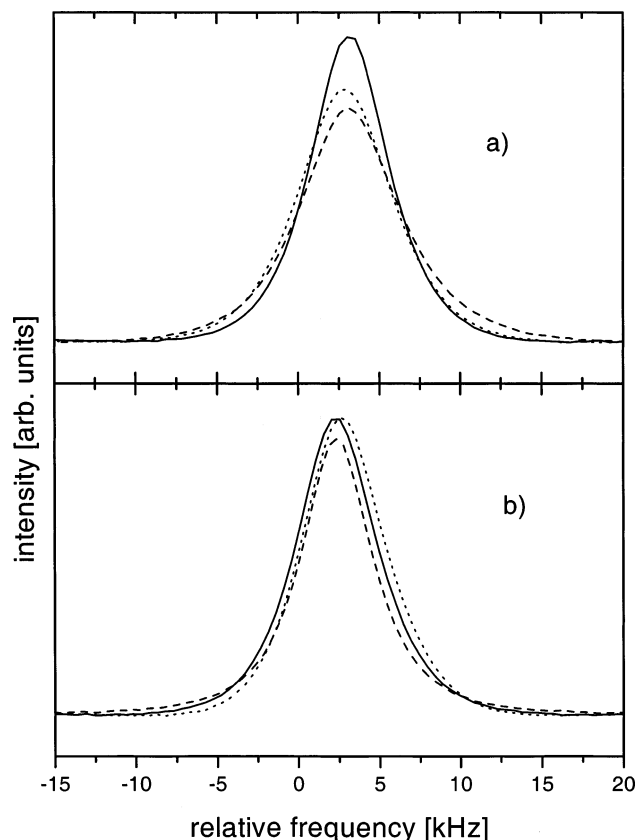


**Figure 1.** Spectra of ionic ferrofluids at different pH values. Grains diameter  $\approx 8$  nm and  $[\text{Fe}] = 0.1 \text{ mol L}^{-1}$ . (a) Alkaline samples: (solid line) pH = 11.5; (dashed line) pH = 10.5; (dotted line) pH = 10.2. (b) Acid samples: (solid line) pH = 2.65; (dashed line) pH = 3.78; (dotted line) pH = 4.52.

ferrofluid); pH = 12, here grains bear negative charges with  $\text{TMA}^+$  counterions (alkaline ferrofluid). The concentration in magnetic material is given by  $[\text{Fe}]$ , total concentration of iron in the sample expressed in  $\text{mol L}^{-1}$  and determined by chemical dosage.<sup>7</sup> The concentration range explored in this study goes from 0.05 to  $2.25 \text{ mol L}^{-1}$ .

**Different pH at Constant  $[\text{Fe}]$  Value.** Samples at different pH values are prepared by adding different quantities of TMAOH to a constant amount of acid ferrofluid,  $[\text{Fe}] = 0.1 \text{ mol L}^{-1}$ . The pH intervals investigated are  $10.2 < \text{pH} < 11.5$  and  $2.65 < \text{pH} < 4.52$ .

**Setup.** The NMR setup is a Bruker-MSL 300 spectrometer with a 7.05 T magnet. The uniformity of the magnetic field is set to better than 0.01 ppm all over of the sample volume by means of conventional shimming coils. Sample temperature is stabilized at  $(295.2 \pm 0.1) \text{ K}$ . The probe is a double bearing CP/MAS with 7 mm spinners.

## Results and Discussions

Proton NMR spectra of alkaline and acid ferrofluids are plotted in Figure 1a,b, respectively. In both sets of samples  $[\text{Fe}]$  is fixed to  $0.1 \text{ mol L}^{-1}$  whereas pH values vary. The spectra of these two series have about the same line width ( $\sim 6 \text{ kHz}$ ) and the same shape. They are practically symmetric and can be well fitted to the convolution of a Gaussian and a Lorentzian function. In alkaline ferrofluids, the half-height width ( $\Gamma$ ) increases from about 5.5 to 7.5 kHz, as the pH comes closer to the PZC. No similar trend is observed in acid ferrofluids. As pointed out above, when pH values come closer to the PZC,<sup>8,9</sup> the grain surface charge density decreases, and consequently, distances

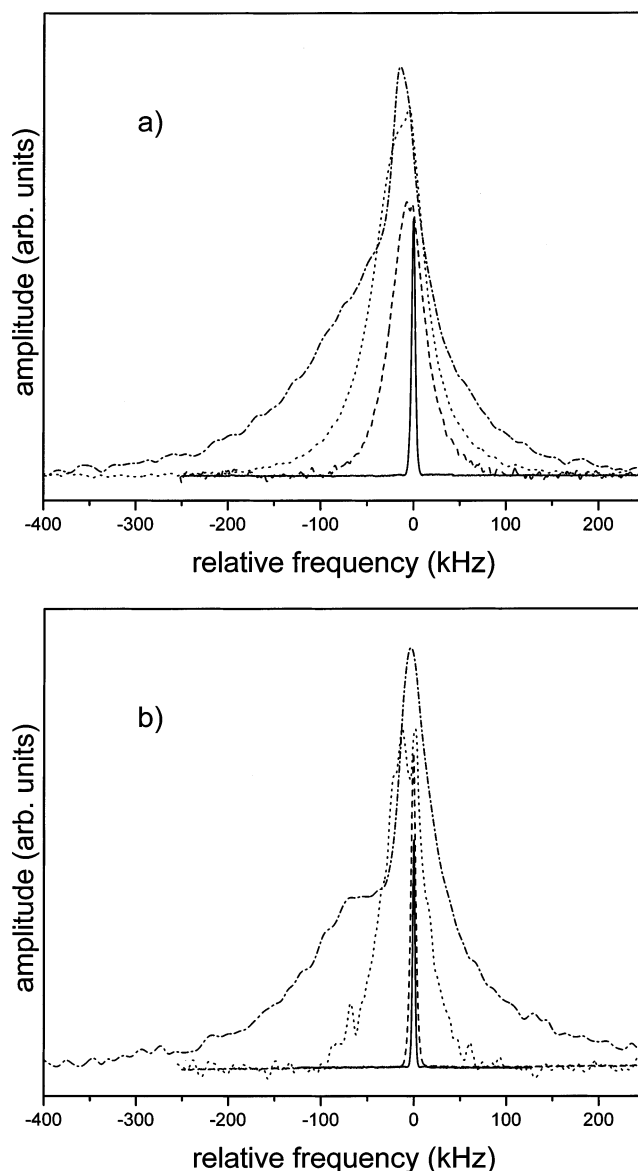


**Figure 2.** Spectra from ionic ferrofluids having different concentrations of magnetic grains (grains diameter  $\approx 8$  nm). (a) pH = 12: (solid line)  $[\text{Fe}] = 0.05 \text{ mol L}^{-1}$ ; (dashed line)  $[\text{Fe}] = 0.1 \text{ mol L}^{-1}$ ; (dotted line)  $[\text{Fe}] = 0.75 \text{ mol L}^{-1}$ ; (dash-dot line)  $[\text{Fe}] = 2.25 \text{ mol L}^{-1}$ . (b) pH = 2.5: (solid line)  $[\text{Fe}] = 0.06 \text{ mol L}^{-1}$ ; (dashed line)  $[\text{Fe}] = 0.5 \text{ mol L}^{-1}$ ; (dotted line)  $[\text{Fe}] = 0.75 \text{ mol L}^{-1}$ ; (dash-dot line)  $[\text{Fe}] = 2.25 \text{ mol L}^{-1}$ .

between grains tend to decrease. As the number of grains is constant, this process could induce the formation of clusters of different sizes and of diluted regions, simultaneously. Water molecules could be trapped within the clusters. However,  $\Gamma$  is not very sensitive to the variation of pH, irrespective to the acid or alkaline character of the sample. This fact is a first indication that NMR line broadening is not a consequence of the electric interactions between water molecules and grains surfaces.

Let us now analyze the water NMR spectra of a series of samples at fixed pH and varying the iron concentration  $[\text{Fe}]$ . Parts a and b of Figure 2 show the 7 T NMR spectra for the alkaline and acid samples, respectively. Spectral shapes change drastically with  $[\text{Fe}]$ . In both series, the NMR lines are roughly symmetric at low  $[\text{Fe}]$ , whereas they become broader and more asymmetric for higher  $[\text{Fe}]$ . Despite the low concentration samples have the narrower spectra, their width ( $\Gamma$ ) is 3 orders of magnitude larger than the one obtained with the same

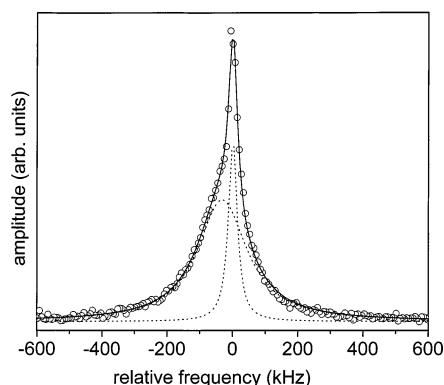


**Figure 3.** (○) NMR spectral results of alkaline sample with  $[\text{Fe}] = 2.25 \text{ mol L}^{-1}$ . (---) Individual fit functions. (—) Superposition of the two Lorentzians.

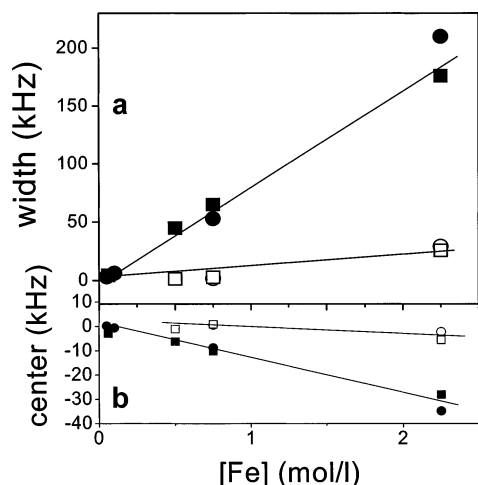


**Figure 4.** Width  $[\Gamma]$  (a) and frequency shift  $[\Delta\nu]$  (b) of the maximum of the individual Lorentzians as a function of the iron concentration in alkaline (circles) and acid (squares) samples (narrow line, open symbols; broad line, full symbols). The solid lines are guides for the eyes.

spectrometer in chemically pure water (5 Hz). At higher  $[\text{Fe}]$ , also a narrower peak arises together with the broad one. Its width also increases with  $[\text{Fe}]$ . In all the samples, the spectra can be fitted by the linear combination of two Lorentzian functions having very different widths and shifted maxima (in the Larmor frequency scale). Figure 3 shows the typical fit of the NMR spectra of an alkaline sample with  $[\text{Fe}] = 2.25 \text{ mol L}^{-1}$ . The relative area of the narrowest component increases (from  $\sim 1\%$  at  $[\text{Fe}] = 0.5 \text{ mol L}^{-1}$  to  $\sim 20\%$  at  $[\text{Fe}] = 2.25 \text{ mol L}^{-1}$ ) as a function of  $[\text{Fe}]$ . The fact that the NMR spectra are composed by two distinct Lorentzian functions suggests that water molecules feel two types of environments, differing on the local averaging of the magnetic field. However, this result *does not depend* on the samples pH, which controls the grains surface charge density and sign. As a conclusion, these different environments should not be simply associated with bulk and surface-bounded water molecules.

Parts a and b of Figure 4 give, for the two sets of samples (acid and alkaline), both the widths ( $\Gamma$ ) and the positions of the maxima ( $\Delta\nu$ ) in the spectra of each Lorentzian component as functions of the iron concentration. Our results show that, within the studied  $[\text{Fe}]$  range,  $\Gamma_{\text{broad}}$  grows about 2 orders of magnitude for all the investigated samples (Figure 4a, full symbols) while  $\Gamma_{\text{narrow}}$  grows with a less steep trend. This fact reinforces, therefore, the assumption that the NMR line width depends only on  $[\text{Fe}]$ . Similarly to  $\Gamma_{\text{narrow}}$ ,  $\Delta\nu_{\text{narrow}}$  remains almost constant

with  $[\text{Fe}]$ . A clear decreasing trend of the spectral position of the broad line center  $\Delta\nu_{\text{broad}}$  for increasing  $[\text{Fe}]$  (Figure 4b, full symbols) is observed. This means that the average internal magnetic field decreases while  $[\text{Fe}]$  increases. This frequency shift shows a linear dependence on the iron concentration, indicating that the net magnetization is proportional to the density of magnetic grains. It is also expected that the increasing of  $[\text{Fe}]$  narrows the orientational distribution function of the grains magnetic moment. Note that for small  $[\text{Fe}]$ , the behaviors of the narrow and broad components of the spectra converge to a unique one (same  $\Delta\nu$  and same  $\Gamma$ ; see Figure 4a,b), thus making difficult the two contributions to be distinguished.

The local magnetic field, within the small interstitial volumes of the ferrofluid, is very inhomogeneous.<sup>4</sup> As interstitial regions are hundreds of Angstroms long, and the magnetic field varies drastically on them, the field gradients attain values many orders of magnitude higher than those available at a laboratory scale. This spatial variation of the local field, due to the presence of magnetic grains, depends on  $[\text{Fe}]$ . While water molecules diffuse translationally through the intergrain volume, the protons feel fluctuating magnetic fields provided by both the water diffusion process and the spatial distribution of magnetic field gradients. Consequently, the resonance frequency offset of water protons,  $\Delta\omega_0(t)$ , is also time dependent. Also this frequency fluctuation should be expected to depend on  $[\text{Fe}]$ .

The spin–lattice ( $T_1$ ) relaxation time and the decay rate of the echo amplitude following the Hahn-echo pulse sequence, were both measured in the acid and alkaline sets of samples. It was not possible to extend this measurement to the samples having the highest iron concentration ( $[\text{Fe}] = 2.25 \text{ mol L}^{-1}$ ) because no saturation condition for protons was achieved. This is due to the extremely broad ( $\leq 1 \text{ MHz}$ ) spectral width. This usual NMR experiment prepares the spin magnetization in an initial state with a saturating RF pulse, the magnetization evolves during a time  $\tau$  and then a read pulse is used to measure the remaining (a relaxed) magnetization. Here the decay rate of the transverse magnetization,  $T_2$ , is due to both spin–spin interactions and the loss of the transverse spin-coherence while the water molecules diffuse through regions with position dependent magnetic fields within the intergrain volume. This procedure restricts our study mainly to the narrow contribution of the NMR spectra because wide NMR lines lose coherence (relax) faster than the narrower ones. In the more concentrated samples the broader contributions attenuate before the read pulse can be triggered. That is, the decay happens in times shorter than those experimentally accessible.

Parts a–c of Figure 5 show the typical behavior of the Hahn-echo decay at three iron concentrations of ionic ferrofluids. In all the analyzed samples  $T_2$  is much shorter ( $\approx 10 \mu\text{s}$ ) than the value found in pure water ( $\approx 0.2 \text{ s}$ ), whereas  $T_1$  is very similar in both cases ( $\approx 1 \text{ s}$ ). The higher concentration profiles,  $[\text{Fe}] = 0.75$  and  $0.5 \text{ mol L}^{-1}$  can be well described by a simple exponential law with a decay time of  $9 \mu\text{s}$ . The lower concentration profiles ( $[\text{Fe}] < 0.5 \text{ mol L}^{-1}$ ) deviate from a single exponential at short times for the basic and acid samples. The whole set of data can be fitted to a more general expression for the Hahn-echo amplitude of a spin system moving randomly in a region of spatially dependent (Gaussian distribution) local fields:<sup>10</sup>

$$E(2\tau) = \exp\left\{-\overline{\Delta\omega_0^2}\tau_c^2\left[4e^{-\tau/\tau_c} - e^{-2\tau/\tau_c} + \frac{2\tau}{\tau_c} - 3\right]\right\} \quad (1)$$

where  $\tau$  is the pulse separation in the Hahn-echo experiment and  $\tau_c$  is a correlation time. This expression comes from the

TABLE 1

sample type	[Fe] (mol L <sup>-1</sup> )	$\tau_c$ ( $\times 10^{-6}$ s)	$\overline{\Delta\omega_0^2}$ ( $\times 10^9$ Hz)	$\overline{\Delta\omega_0^2\tau_c^2}$	$\zeta$ (Å)	$d$ (Å)
A	0.06	$10.0 \pm 0.3$	$1.45 \pm 0.02$	0.15	1414	850
A	0.1	$4.6 \pm 0.1$	$8.6 \pm 0.1$	0.18	959	715
A	0.5	$0.7 \pm 0.2$	$157 \pm 3$	0.08	379	418
A	0.75	$0.4 \pm 0.1$	$190 \pm 5$	0.04	301	365
B	0.05	$7.1 \pm 0.3$	$2.7 \pm 0.1$	0.15	1215	901
B	0.1	$5.0 \pm 0.1$	$5.3 \pm 0.7$	0.12	974	715
B	0.75	$0.5 \pm 0.1$	$533 \pm 6$	0.15	327	365

<sup>a</sup> The first column to the left indicates the acid (A) or alkaline (B) class of ferrofluids, and the second column contains the iron concentration of each sample. The third and fourth columns show the fitting parameters to eq 1, whereas the fifth column measures the departure of the fluctuation motions from the slow (or fast) limits; see text. The two columns on the right compare the calculated intergrain distance  $d$  by assuming a homogeneous hcp structure, and the correlation length  $\zeta$  due to diffusion.

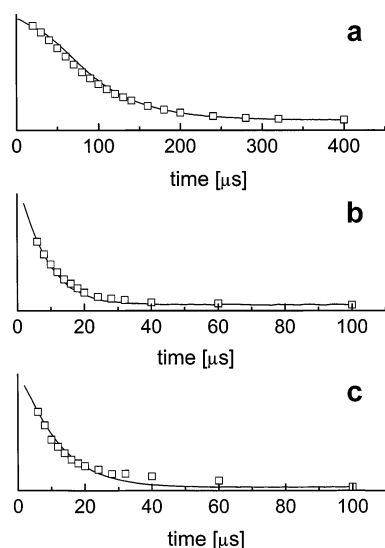


**Figure 5.** Evolution of the Hahn-echo amplitude with the pulse separation (squares) and FID signals (solid lines) for different iron concentrations. Acid samples, pH = 2.5: (a) [Fe] = 0.06 mol L<sup>-1</sup>; (b) [Fe] = 0.5 mol L<sup>-1</sup>; (c) [Fe] = 0.75 mol L<sup>-1</sup>.

Anderson–Weiss theory, where a correlation function  $g_\omega(\tau) = \exp[-|\tau|/\tau_c]$  is assumed for the fluctuating frequency offset.<sup>10,11</sup> The correlation time  $\tau_c$  characterizes the rate of the frequency offset fluctuations:

$$\tau_c = \int_0^\infty \frac{\Delta\omega_0(t) \Delta\omega_0(t - \tau)}{\overline{\Delta\omega_0^2}} d\tau$$

and the mean square frequency fluctuation  $\overline{\Delta\omega_0^2}$  is the second moment of the resonance line. Table 1 shows  $\tau_c$  and  $\overline{\Delta\omega_0^2}$  obtained from the best fits of data to eq 1. The relative magnitude of these parameters defines: (i) the rapid fluctuations or *motional narrowing* limit when  $\overline{\Delta\omega_0^2}\tau_c^2 \ll 1$  and (ii) slow fluctuations or *slow-motion* limit when  $\overline{\Delta\omega_0^2}\tau_c^2 \gg 1$ . This quantity is also presented in Table 1. It ranges from 0.04 to 0.18, indicating that all the samples are in an intermediate regime neither the fast nor the slow limit.

The echo attenuation profiles coincide with the free induction decay signals (FID) at all concentrations shown in Figure 5. The fact that after the FID has decayed no refocusing occurs could indicate that it corresponds to the fast motion limit, which is related to homogeneous line shapes. On the contrary, at higher

concentrations, the spectra are definitely asymmetric (and even structured), corresponding, therefore, to an inhomogeneous spectrum.

The correlation length due to diffusion,  $\zeta$ , is defined by  $\sqrt{\tau_c D}$ , where  $D$  is the diffusion coefficient. The values of  $\zeta$  shown in Table 1 were calculated from the  $\tau_c$  values of the narrow components of the spectra and  $D$  was taken equal to that of pure water ( $D = 2 \times 10^{-9} \text{ m}^2 \text{ s}^{-1}$ ). These numbers can be compared with the mean distance ( $d$  in Table 1) between magnetic grains calculated at different [Fe], assuming a homogeneous hcp grains distribution. The numbers in these two columns are similar, suggesting that both the homogeneous distribution of magnetic grains and the value adopted for the water diffusion coefficient are compatible with our observation at the lower iron concentrations.

The combination of these two studies (Hahn-echo and NMR spectra) leads to the conclusion that water molecules, resonating in the narrow NMR band, are located in a magnetic environment characterized by a homogeneous distribution of magnetic grains. The remaining broad band contribution cannot be explained in a similar way, due to its asymmetric characteristics. This behavior can only be found in the slow motions regime, where molecular diffusion is not fast enough to average the spatial inhomogeneities of the local fluctuations of the frequency offsets. This result could be interpreted by assuming an increase of the mean distance between the *magnetic units*. As the line broadening is more noticeable at higher [Fe], we will assume that such *magnetic units* are made of *grain aggregates*. This type of cluster (which has the shape of needles or even bundles) was already observed in some particular situations<sup>12,13</sup> where ferrofluids are subjected to magnetic fields. Structured spectra, as the one shown in Figure 3, where only 80% of water protons belong to the broader component of the NMR spectrum and 20% to the narrower component, should be originated by water molecules that experience two types of magnetic environments. Our results indicate that the ionic magnetic colloid, in the presence of the 7 T magnetic field, experiences a small scale agglomeration process, which depends on the sample iron concentration: the greater [Fe], the stronger the agglomeration process. Although less evident from the NMR spectra, this behavior should also be present at lower concentrations. In this inhomogeneous spatial distribution of magnetic grains there would exist regions with smaller grains concentration, where the frequency offset fluctuations are slower than the one in the more highly concentrated regions.

**Acknowledgment.** We thank SECYT Universidad Nacional de Córdoba and CONICET from Argentina, COFECUB, FAPESP, PRONEX/CNPq from Brazil and COFECUB, CNRS from France for financial support.

## References and Notes

- (1) Rosensweig, R. E. *Ferrohydrodynamics*; Cambridge University Press: Cambridge, U.K., 1985.
- (2) *Magnetic Fluids and Applications Handbook*; Berkovski, B., Bashtovoy, V., Eds.; Begell House: Wallingford, U.K., 1996.
- (3) Massart, R. C. R. *Acad. Sci. Paris* **1980**, 291C, 1.
- (4) González, C. E.; Pusiol, D. J.; Figueiredo Neto, A. M.; Ramia, M.; Bee, A. *J. Chem. Phys.* **1998**, 109, 4670.
- (5) Bacri, J. C.; Perzynski, R.; Salin, D.; Cabuil, V.; Massart, R. *J. Magn. Magn. Mater.* **1990**, 85, 27.
- (6) Bee, A.; Massart, R.; Neveau, S. *J. Magn. Magn. Mater.* **1995**, 149, 6.
- (7) Charlot, G. *Les Méthodes de la Chimie Analytique*; Masson & Cie Ed.: Paris, 1966; p 737.

- (8) Jolivet, J. P. In *De la Solution à l'oxide*; CNRS Edition: Paris, 1994.
- (9) Hasmonay, E.; Bee, A.; Bacri, J. C.; Perzynski, R. *J. Phys. Chem. B* **1999**, *103*, 6421.
- (10) Callaghan, P. T. *Principles of Nuclear Magnetic Resonance Microscopy*; Clarendon Press: Oxford, U.K., 1993; p 414.
- (11) Kimmich, R. *NMR—Tomography, Diffusometry, Relaxometry*; Springer-Verlag: Berlin, Heidelberg, 1997.
- (12) Matuo, C. Y.; Tourinho, F. A.; Figueiredo Neto, A. M. *J. Magn. Mater.* **1993**, *122*, 53.
- (13) da Silva, M. F.; Figueiredo Neto, A. M. *Phys. Rev. E* **1993**, *48*, 4483.